





Late Pliocene variability of the Agulhas Current: Planktic foraminiferal records from southwest Indian Ocean

Rahul Dwivedi ¹, Vikram Pratap Singh ^{1,*}, Shivani Pathak ¹, Kirti Ranjan Mallick ², Pravat Kumar Nayak²

¹Department of Geology, Indira Gandhi National Tribal University, Amarkantak, Madhya Pradesh, India

²PG Department of Geology, Utkal University, Bhubaneswar, Odisha, India

ABSTRACT

The Pliocene climate was punctuated by many global glacial events, which set the stage for the Quaternary glaciations. The Late Pliocene witnessed two major glacial events, at 3.3 and 2.7 Ma. These events changed not only the dynamics of the ice sheets and global climate but also the ocean circulation patterns. The present work aims to reconstruct the variations in the strength of the Agulhas Current (AC) during the Late Pliocene on the basis of the planktic foraminiferal census and stable oxygen isotope data from IODP Hole U1474A. The relative abundance of the Indian Ocean Group (IOG), the Southern Ocean Group (SOG) and the productivity indicators (PI) show significant variations, recording a change in the AC strength. The stable oxygen isotope also corroborates the variation in the Sea Surface Temperature (SST), in response to the AC strength. The records indicate five episodes of weakening of the AC during the Late Pliocene, which were in response to the waxing Antarctic Ice Sheet leading to the northward migration of the polar fronts.

ARTICLE HISTORY

Received 20 November 2024

Revised 4 December 2024

Accepted 5 December 2024

<https://doi.org/10.5281/zenodo.14279620>

KEYWORDS

Agulhas Current
Late Pliocene
Planktic Foraminifera
Antarctic Ice Sheet
Antarctic Polar Fronts
Oxygen isotope
Glacial events

1. INTRODUCTION

The Late Pliocene Epoch (3.6-2.6 My) witnessed a significantly warm global climate. The period from 3.3 to 2.9 Ma, also known as the mid-Piacenzian Warm Period (mPWP), saw the global average temperature almost 3–4°C warmer than today (Fedorov et al., 2013; Haywood et al., 2013; Jiménez-Moreno et al., 2019). The Late Pliocene interval was not only significantly warm but also witnessed episodes of significant glaciations (De Schepper et al., 2014; Jiménez-Moreno et al., 2019; McClymont et al., 2023), which led to the initiation of the Quaternary glaciations (Westerhold et al., 2020).

The Late Pliocene began with the onset of the Northern Hemisphere Glaciation (NHG) at 3.6 Ma

(Ravelo et al., 2004) evidences of which can be found in the substantial waxing of North American Ice Sheet at 3.5 Ma (Gao et al., 2012). Other than this, two major glacial events have also been reported at 3.3 and 2.7 Ma (De Schepper et al., 2014).

The 3.3 Ma event, corresponding to MIS M2 (Lisiecki and Raymo, 2005; Tan et al., 2017), was a global event, which caused a major decline in the sea surface temperatures of the North Atlantic (De Schepper et al., 2013) and led to glacial expansion in the Northern Hemisphere (Jansen et al., 2000; Kleiven et al., 2002) as well as a significant waxing of the Antarctic Ice Sheet (AIS) (Brigham-Grette et al., 2013).

The evidence for the 2.7 Ma glacial event has been recorded in the abrupt increase in the ice-rafted

*Corresponding author. Email: vikram.singh@igntu.ac.in (VPS)

debris (IRD) in the northern high latitudes (Beal et al., 2011; Teschner et al., 2016). These records also indicate the intensification of the NHG (iNHG) during this period (McClymont et al., 2023). This event is also recorded in the Southern Ocean, which indicate a marked sea-ice expansion and progressive waxing of the AIS during the latest Pliocene (Hillenbrand and Ehrmann, 2005; Naish et al., 2009), leading to a bipolar expansion of the ice sheets.

These two glacial events were punctuated by the mPWP (De Schepper et al., 2014; Haywood et al., 2016; de la Vega et al., 2020; McClymont et al., 2023). The mPWP caused a significant reduction in the polar ice caps in both the hemispheres (Hill et al., 2007; Dolan et al., 2011) and raised the global annual mean temperatures (Haywood et al., 2009; Dowsett et al., 2012; Lunt et al., 2012). It has been considered as one of the best analogues to study the modern climate and future climate projections (Haywood et al., 2016).

The climatic variations and changing extent of the polar ice sheets would have profound impact on the ocean circulation in the mid-latitudes. The AIS has a large impact on the position of the Antarctic Polar Fronts (APF), causing them to migrate northward during the glacial events (Kemp et al., 2010; Taylor-Silva and Riesselman, 2018). The northward migration of the APF allows the incursion of the cold Southern Ocean waters to the sub-tropical latitudes, thereby influencing the surface ocean currents at the mid-latitudes (Singh et al., 2023). The Agulhas Current (AC), which is the largest western boundary current (Simon et al., 2013), is one such current which has been impacted a lot by the migrating APF.

The AC, carrying ~70 Sverdrup (Sv) of water (Simon et al., 2013), is a major source of warm water to the southern Atlantic Ocean, and also feeds the returning arm of the global ocean conveyor belt (Beal et al., 2011). The strength of the AC was impacted several times during the Quaternary by the migration of the APF, mainly the subtropical front (STF) (Bard and Rickaby, 2009; Beal et al., 2011; Caley et al., 2014; Nirmal et al., 2023; Singh et al., 2023). Considering the principle of uniformitarianism, we presume that the AC would also have been impacted during the Late Pliocene glacial events which caused the migration of the APF.

In the present study, we have reconstructed the paleoceanography of the AC during the Late Pliocene

using the planktic foraminiferal census and stable isotopic records. The planktic foraminifera, owing to latitudinal provincialism (Bé, 1977), are excellent proxies for reconstructing past circulation patterns. Their stable isotope composition has been largely used as a tool for deciphering the changing SST. The reduction in the AC will be marked by the increase in the abundance of cold water forms due to incursion of cold Southern Ocean water.

The present study focuses on identifying the events of variations in the AC during the Late Pliocene using the relative abundance of planktic foraminifera and stable oxygen isotopic ratio. The AC, being a warm current, will be dominated by the tropical–subtropical planktic foraminiferal species when it is stronger. Any event of reduced strength would be represented by an increase in the relative abundance of cold water species. In the present study, we present the census and stable oxygen isotope records of relevant planktic foraminiferal species recovered from the deep sea sediments from the IODP Hole U1474A from the SW Indian Ocean. The tropical–subtropical species are indicative of the warmer AC, while the temperate and subpolar species indicate the incursion of cold Southern Ocean sourced waters. We have compared the census records with the stable oxygen isotope records from the IODP Hole U1474A as well as the LR04 benthic stack (Lisiecki and Raymo, 2005).

2. STUDY AREA

The IODP Hole U1474A, located in the path of the AC (31°13.00'S; 31°32.71'E; Fig. 1) (Hall et al., 2017), is an ideal site for studying the variability of this current. The pelagic sediments from the deep sea core recovered from this site consist of well-preserved planktic foraminiferal assemblage characterized by a mixture of tropical–subtropical, temperate, and subpolar species.

The AC transports 70 Sv of water, which is derived from the Madagascar Current, Mozambique Current and the recirculated part of the Agulhas Return Current (Fig. 1) (Lutjeharms, 2006). This warm current exerts a significant impact on the global thermohaline circulation by feeding the returning arm of the conveyor belt in the South Atlantic through the Agulhas Leakage (AL) (Zahn et al., 2010).

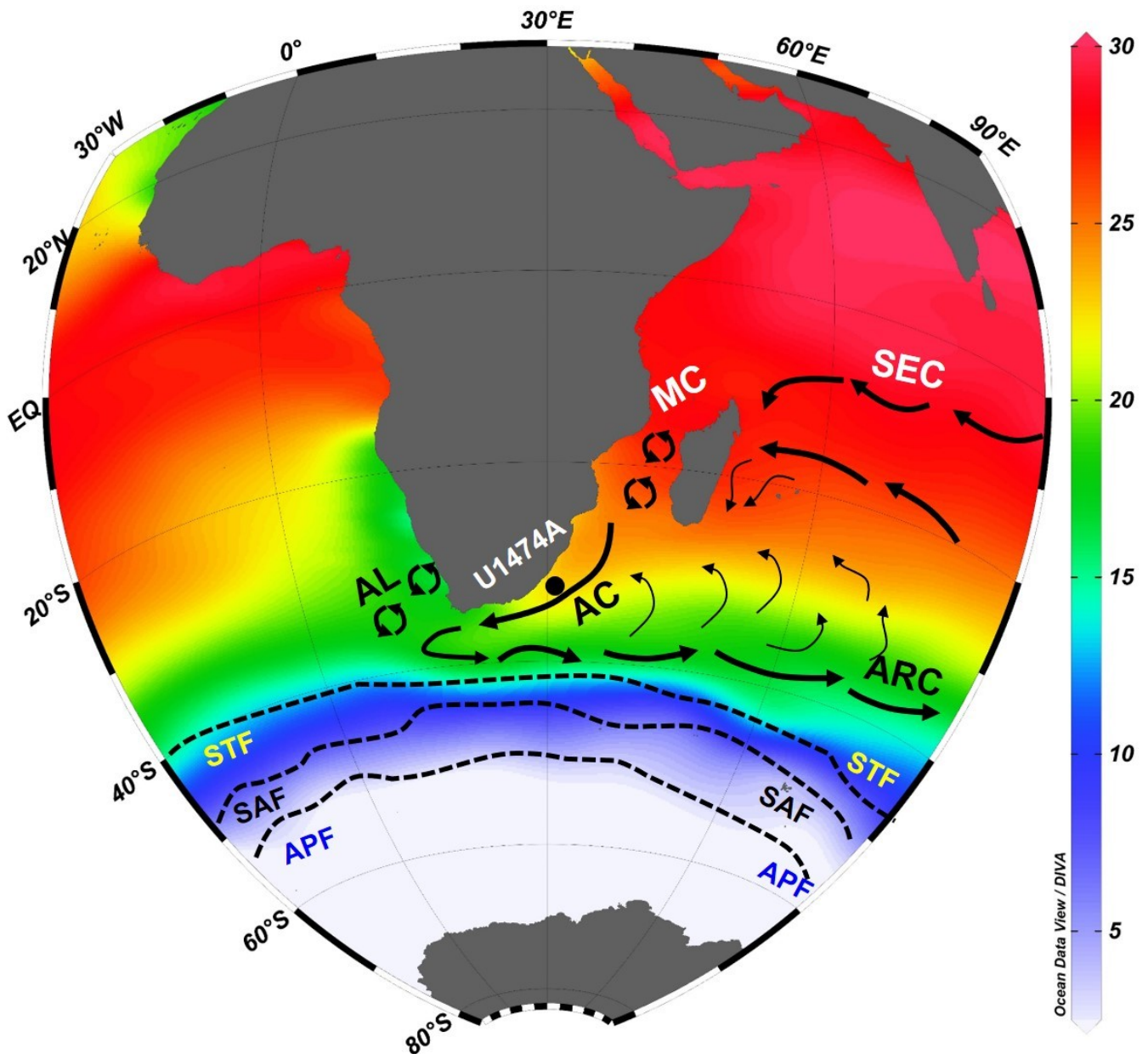


Fig. 1. Modern ocean circulation of the SW Indian Ocean and the location of the study area. The study area is marked by a solid circle. The position of the various Antarctic Polar Fronts is marked after Orsi et al. (1995). Abbreviations: AC - Agulhas Current; AL - Agulhas Leakage; ARC - Agulhas Return Current; MC - Mozambique Current; SEC - South Equatorial Current; STF - Sub Tropical Front, SAF- Sub Antarctic Front, APF- Antarctic Polar Front, SACCF- Southern ACC Front, SBF- Southern Boundary Front. The SST map is compiled from World Ocean Atlas 18 (Locarini et al., 2018) and drawn using Ocean Data View software version 5.6.3 in the orthographic equatorial projection (Schlitzer, 2022).

3. MATERIALS AND METHODS

3.1. Planktic foraminiferal census count data

We processed 130 deep sea samples using wet-sieving method to extract $>150\ \mu\text{m}$ fraction of planktic foraminifera. The taxonomic identification was done up to species level following the taxonomy by Kennett and Srinivasan (1983), Schiebel and Hem-

leben (2017) and Lam and Leckie (2020). The census count data in percentage was generated and relative abundance curves for the key species were plotted.

3.2. Stable Isotope Analysis

Stable oxygen isotope analysis was conducted on the surface dweller *Globigerinoides quadrilobatus*. We picked 4 to 5 ultrasonically cleaned specimens of this

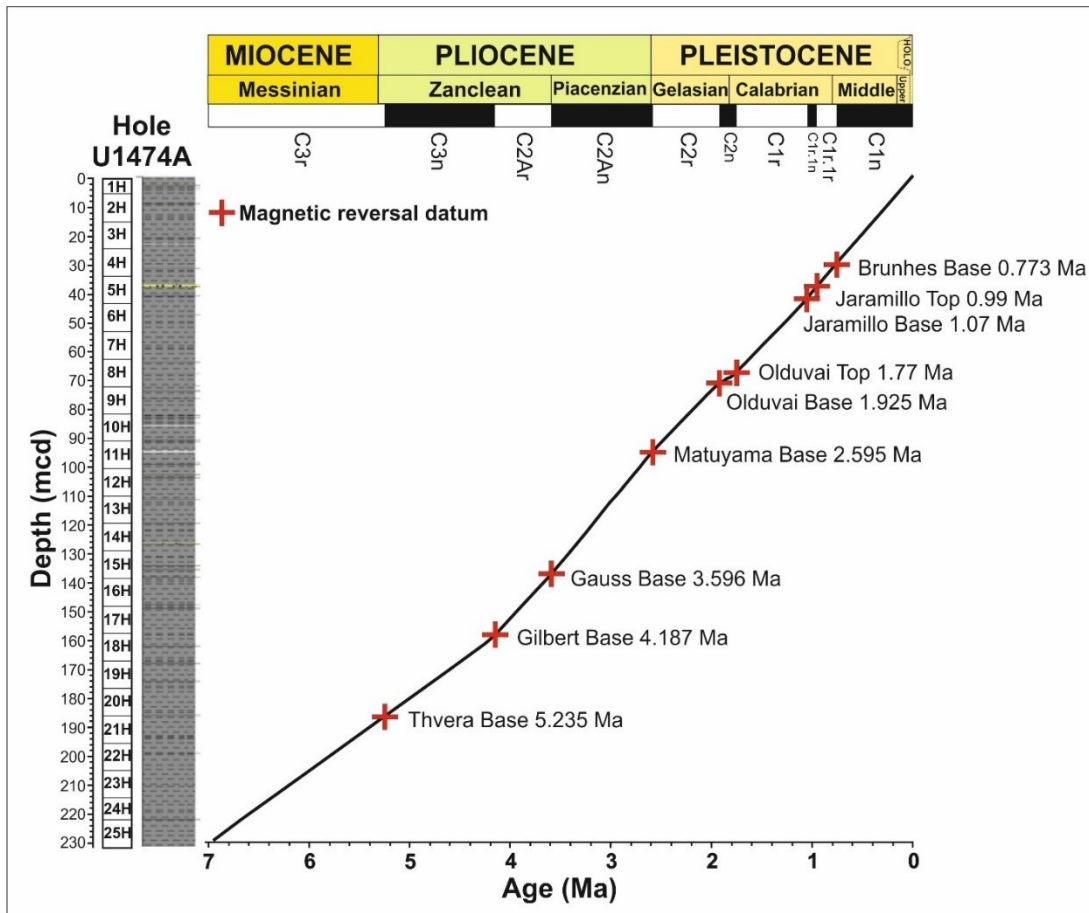


Fig. 2. Age–depth plot of the IODP Hole U1474A. Paleomagnetic stratigraphy after Hall et al. (2017) and revised ages after Ogg (2020).

species from the samples. *Globigerinoides quadrilobatus* is a mixed layer dweller (Chaisson and Ravelo, 1997) and can be used for isotopic analysis of the surface water, as it records the isotopic ratio of ambient shallow water. The stable isotopic analysis was carried out using Kiel IV Carbonate device and Thermo MAT 253 Plus isotopic ratio mass spectrometer device at IISER Kolkata. The oxygen isotope data is reported in δ notation relative to VPDB, with a standard deviation of ± 0.02 ‰.

3.3. Age Model

The age model for the studied core was derived on the basis of the detailed magnetostratigraphy of IODP Hole U1474A (Hall et al., 2017). The absolute ages for palaeomagnetic events and reversal boundaries were taken from Ogg (2020). We calculated the rate of sedimentation by assuming a uniform rate of sedimentation between recorded paleomagnetic reversal events. It was then interpolated to calculate the ages for each sample (Fig. 2). Thereafter, we selected

the samples spanning 2.6 to 3.6 Ma for the present study.

3.4. Planktic Foraminiferal Species Groups for Paleooceanographic Reconstruction

We encountered a total of 60 planktic foraminiferal species, comprising a mixture of tropical, subtropical and temperate forms. Although the planktic foraminiferal assemblage is dominated by the warm water species, it also shows a considerable rise in the population of the cold water forms as well as species preferring eutrophic conditions, indicating a remarkable degree of fluctuation in the relative abundances of the climatically sensitive species.

Considering the ecological preferences and the biogeographical distribution of planktic foraminiferal species (Bé, 1977) and a relative abundance of 5% in at least 10 samples, three main groups of the planktic foraminifera were formed, the Indian Ocean Group (IOG), the Southern Ocean Group (SOG) and Pro-

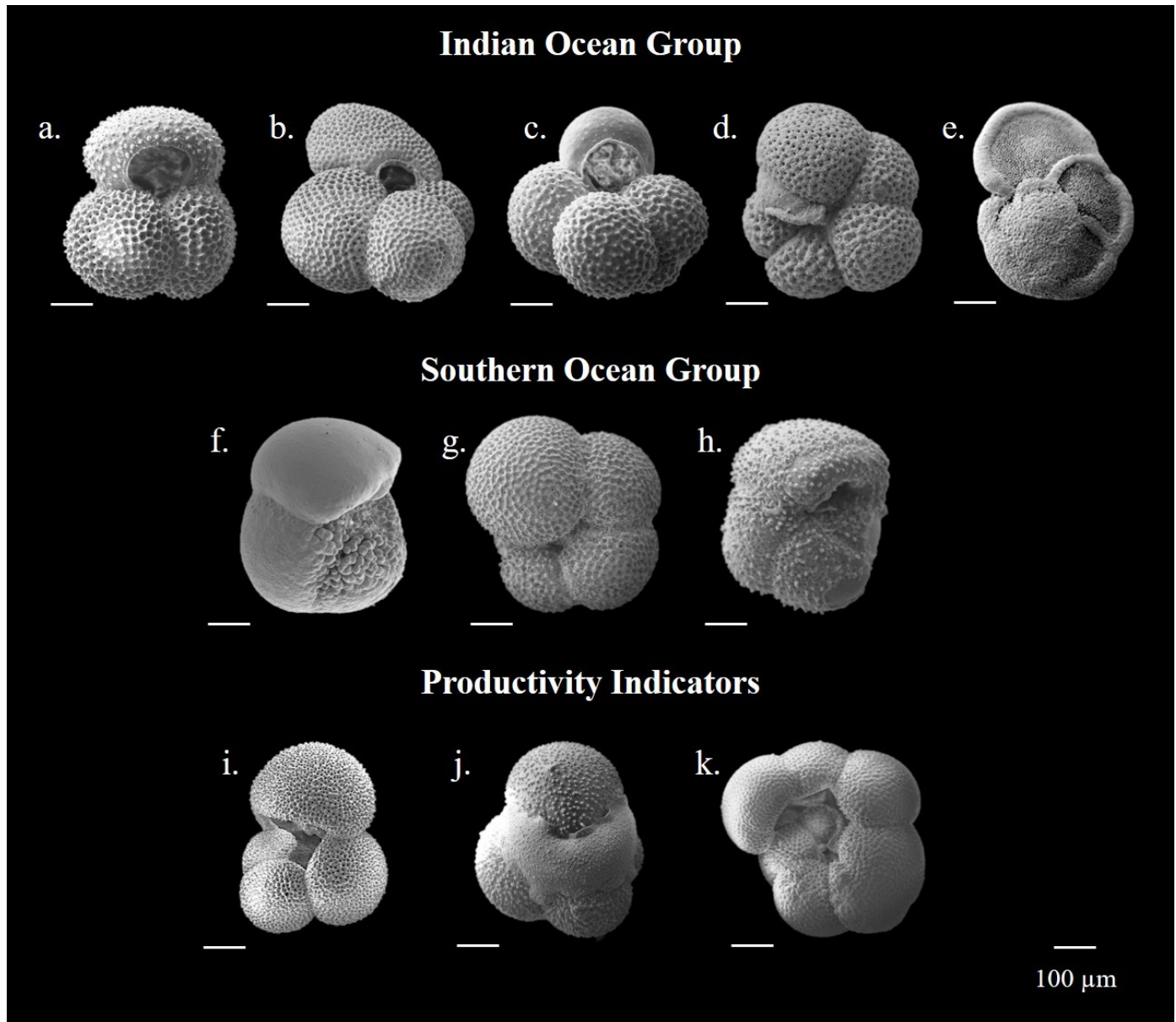


Fig. 3. Planktic foraminiferal groups formulated for the reconstruction of the AC. Indian Ocean Group comprises of: a. *Globigerinoides ruber*, b. *Trilobatus sacculifer*, c. *Globoturborotalita rubescens*, d. *Neogloboquadrina acostaensis*, e. *Menardella menardii*; Southern Ocean Group comprising of: f. *Globoconella inflata*, g. *Neogloboquadrina incompta*, h. *Globoconella puncticulata*; Productivity Indicators consisting of: i. *Globigerina bulloides*, j. *Globigerinita glutinata*, k. *Neogloboquadrina dutertrei*. The SEM images are of planktic foraminiferal species from IODP Hole U1474a. The scale bar represents a scale of 100 µm. The taxonomic identification is after Kennett and Srinivasan (1983), Schiebel and Hemleben (2017) and Lam and Leckie (2020). The SEM was conducted at Ravenshaw University using Zeiss Gemini 300 Scanning Electron Microscope.

ductivity Indicators (PI) (Fig. 3). The IOG comprises the tropical–subtropical water-dwelling species *Globigerinoides ruber*, *Trilobatus sacculifer*, *Globoturborotalita rubescens*, *Neogloboquadrina acostaensis*, and *Menardella menardii*. The SOG comprises cold temperate, subpolar species *Globoconella inflata*, *Globoconella puncticulata*, and *Neogloboquadrina incompta*, and the PI includes *Globigerinita glutinata*, *Globigerina bulloides* and *Neogloboquadrina dutertrei*.

4. RESULTS

The studied time interval (3.6 to 2.6 Ma) has been divided into three main events: i. pre-mPWP (3.6 to 3.3 Ma), ii. mPWP (3.3 to 2.9 Ma), and iii. Post-mPWP (2.9 to 2.6 Ma). The entire Late Pliocene interval at Hole U1474A saw significant variations in the planktic foraminiferal relative abundance (Fig. 4). The correlation of the relative abundance of IOG, SOG and PI, and the stable oxygen isotope ratio indi-

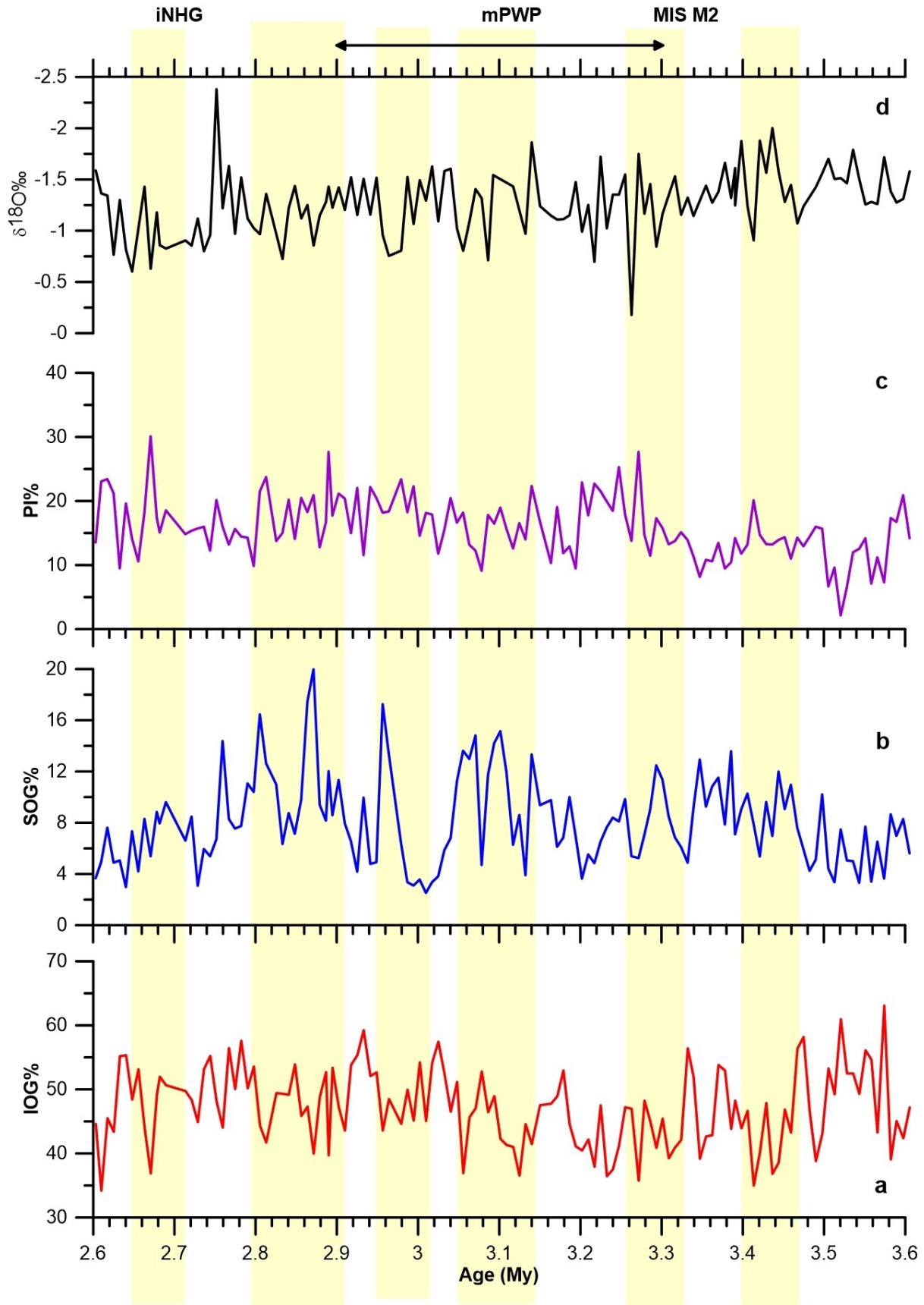


Fig. 4. The relative abundances of the planktic foraminifera from IODP Hole U1474A: a. Indian Ocean Group (IOG); b. Southern Ocean Group (SOG); c. Productivity Indicators (PI), correlated with d. $\delta^{18}O$ of *Globigerinoides quadrilobatus* from U1474A. The shaded portions indicate the intervals of decline in IOG which indicate reduction in the strength of the AC.

icates the shifting of the ecotones, thereby indicating the variation in the strength of the AC.

The IOG showed significant variations during the Late Pliocene, marking six events of marked decline in the relative abundance. The pre-mPWP interval (3.6 to 3.3 Ma) started with a high abundance of IOG, which showed a decline from 60% to 35% between 3.5 to 3.4 Ma (Fig. 4a). These events are corroborated by an 8–10% rise in the relative abundance of the SOG when it reached >14% (Fig. 4b) of the total faunal composition. The PI showed an increase to comprise almost 20% (Fig. 4c), along with a positive excursion in $\delta^{18}\text{O}$ values (Fig. 4d). The IOG then gradually increased after 3.4 Ma to reach 60% at 3.34 Ma. During this interval, the SOG declined severely to less than 5%. The average abundance of IOG declined significantly between 3.3–3.28 Ma (by 25%) while the SOG increased to ~15% and the PI also showed higher abundance. The $\delta^{18}\text{O}$ during this interval showed positive excursion, to reach the highest value. The interval between 3.27 to 2.9 Ma showed constantly higher abundance of IOG, and substantial decline in SOG. Although there were two pulses of rise in SOG, these seem to be in response to the local hydrographic changes. These two events at 3.14–3.05 Ma and 2.97–2.95 Ma saw a rise of ~15% in SOG, slight rise in PI and positive excursion in $\delta^{18}\text{O}$. Post the mPWP interval, the SOG showed the highest abundance to reach 20% of the total faunal population between 2.88–2.8 Ma, while the IOG declined by almost 10% during this interval. There was slight positive excursion in the $\delta^{18}\text{O}$ values. Another event of decline in IOG was observed at 2.68 Ma, where the abundance decreased by almost 20%. Interestingly, this event didn't show significant rise in the SOG, but the PI rose to 30% of the total faunal population indicating enhanced productivity. This event also saw a positive excursion in the $\delta^{18}\text{O}$ from 2.75 to 2.68 Ma.

The intervals showing a decline in the relative abundance of IOG, and corresponding higher abundance of SOG are associated by a positive excursion in the $\delta^{18}\text{O}$ values from Hole U1474A, indicating lower SST, marking an incursion of the cold, Southern Ocean-sourced waters to the IODP Hole U1474A.

5. DISCUSSION

Although the Pliocene Epoch was a period of significantly warm climate, it witnessed significant glaciations in both hemispheres prior to the Qua-

ternary Period (De Schepper et al., 2014). The geological records provide detailed evidence of globally recognised glacial events during the Pliocene (De Schepper et al., 2014).

The planktic foraminiferal records from Hole U1474A also indicate the variations in the AC under the impact of these events during the Pliocene. The interval from 3.6 to 2.6 Ma showed a consistently high abundance of the IOG, but there were six events of rise in SOG observed during this period, which were also corroborated by an increase in the PI as well as positive excursion in $\delta^{18}\text{O}$. We believe that these events occurred due to a weakening of the AC in response to northward migration of the APF, that caused the influx of cold Southern Ocean waters.

The Late Pliocene (3.6 My onwards) began with a higher IOG, marking a stronger AC due to the southwardly positioned APF under the impact of reduced AIS. The AIS was severely reduced and the SST of the Southern Ocean was significantly warmed between 3.6 and 3.4 Ma (Naish et al., 2009; McKay et al., 2012; Levy et al., 2012). The AC would have been significantly stronger during this interval, although there were pulses of rise in SOG indicating reduced flow.

The Early Pliocene warmth was terminated by a glacial event at 3.3 Ma (MIS M2) (Lisiecki and Raymo, 2005; De Schepper et al., 2014). The oxygen isotope values from U1474A also exhibit a sharp positive excursion, indicating the influence of this glacial event on the AC. The 3.3 Ma event, which was a major global glaciation (McKay et al., 2012; Brigham-Grette et al., 2013; Andreev et al., 2013), would have caused the waxing of the AIS, leading to a northward migration of the APF. The IOG declined significantly from 3.3 Ma and reached to the minimum abundance at 3.28 Ma. The 3.3 Ma glacial event caused a marked reduction in the AC.

The 3.3 Ma glacial event was followed by the mPWP, when the Antarctic and Greenland ice sheets became smaller than the present (Hill et al., 2010; Dolan et al., 2011). The impact of the mPWP substantially reduced the AIS, which would have restricted the APF to the southern latitudes, thereby strengthening the AC from 3.3 to 3 Ma. Although there are two events of increased SOG, indicating a reduction in AC for a short interval, we believe that these events warrant further analysis to ascertain their causes, as at the present moment we are unable to explain their cause. The census data of

the IOG and the oxygen isotope values corroborate the warmer conditions and stronger AC during the mPWP interval.

Post mPWP, the glacial conditions that initiated at 2.8 Ma (MIS G10) (Martinez-Boti et al., 2015), led to a high latitude cooling during the Late Pliocene (McClymont et al., 2016), which caused the continuous expansion of the ice sheets (De Schepper et al., 2014). The IOG showed a major decline of ~20% during this interval, while there was a slight increase rise in SOG and a significant rise in PI. Probably the reduced AC allowed the fertile cold waters from the Southern Ocean to reach the study area. Before the onset of Quaternary, a major glaciation occurred at 2.7 Ma (MIS G6/G4) (De Schepper et al., 2014), which led to the intensification of the NHG (McClymont et al., 2016). It was a global event, more pronounced in the NH (Bartoli et al., 2006; Darby, 2008; Knies et al., 2009). The ice core records from Antarctica indicate an extensive cooling during the latest Pliocene in the SH (Naish et al., 2009). These records indicate the vast extent of the 2.7 Ma cooling event. At U1474A, the IOG significantly reduced between 2.7–2.65 Ma, indicating a reduced AC. The SOF during this event increased by 10%, while the oxygen isotope shows a positive excursion, indicating the lowering of the SST. This event also showed enhanced productivity.

6. CONCLUSIONS

The paleoceanographic reconstruction of the AC on the basis of the planktic foraminiferal census data and stable oxygen isotope revealed significant variations in the strength of the Agulhas Current during the Pliocene Epoch. The data reveals five events of significant decline in the strength of the Agulhas Current during the Late Pliocene, at 3.48–3.4 Ma, 3.3–3.2 Ma, 3.1 Ma, 2.9–2.8 Ma and 2.7–2.65 Ma. These events were in response to the glaciations that severed the warm Pliocene climate. The glaciation enhanced the Antarctic Ice Sheet, causing a northward migration of the Antarctic polar fronts which caused significant reduction in the Agulhas Current and incursion of cold Southern Ocean sourced water at the IODP Hole U1474A.

ACKNOWLEDGEMENTS

The authors thank the National Centre for Polar and Ocean Research (NCPOR)-IODP India, Goa

for providing financial assistance for this work (Grant No.: NCPOR/IODP/E.3947/2021). RD thanks NCPOR for the financial support in the form of JRF. SP was financially supported by the Non-NET fellowship from IGNTU. The IODP Hole U-1474A core samples were acquired by VPS from the IODP Kochi Core Centre Japan (request no. #85276IODP). VPS, SP and RD thank IGNTU for the lab facilities and logistic support. KRM and PKN thankfully acknowledge the Utkal University. We are thankful to Prof. Prasanta Sanyal for extending lab facilities for conducting stable oxygen isotope analyses.

References

- Andreev, A.A., Tarasov, P.E., Wennrich, V., Raschke, E., Herzschuh, U., Nowaczyk, N.R., Brigham-Grette, J., Melles, M., 2013. Late Pliocene and early Pleistocene environments of the north-eastern Russian Arctic inferred from the Lake El'gygytyn pollen record. *Climate of the Past Discussions* 9, 4599–4653. <https://doi.org/10.5194/cp-10-1017-2014>.
- Bard, E., Rickaby, R.E.M., 2009. Migration of the subtropical front as a modulator of glacial climate. *Nature* 460, 382–383. <https://doi.org/10.1038/nature08189>.
- Bartoli, G., Sarnthein, M., Weinelt, M., 2006. Late Pliocene millennial-scale climate variability in the northern North Atlantic prior to and after the onset of Northern Hemisphere glaciation. *Paleoceanography* 21, 4205. <https://doi.org/10.1029/2005PA001185>.
- Bé, A.W.H., 1977. An ecological zoogeographic and taxonomic review of recent planktonic foraminifera, in: Ramsay, A.T.S. (Ed.), *Oceanic Micropaleontology*. Academic Press, London. volume 1, p. 1–100.
- Beal, L.M., De Ruijter, W.P.M., Biastoch, A., Zahn, R., 2011. On the role of the Agulhas system in ocean circulation and climate. *Nature* 472, 429–436. <https://doi.org/10.1038/nature09983>.
- Brigham-Grette, J., Melles, M., Minyuk, P., Andreev, A., Tarasov, P., Deconto, R., Koenig, S., Nowaczyk, N., Wennrich, V., Rosen, P., Haltia, E., Cook, T., Gebhardt, C., Meyer-Jacob, C., Snyder, J., Herzschuh, U., 2013. Pliocene warmth, polar amplification, and stepped Pleistocene cooling recorded in NE Arctic Russia. *Science* 340, 1421–1427. <https://doi.org/10.1126/science.1233137>.
- Caley, T., Peeters, F.J., Biastoc, A., Rossignol, L., Sebille, E., Durgadoo, J., Malaizé, B., Giraudeau, J., Arthur, K., Zahn, R., 2014. Quantitative estimate of the paleo-Agulhas leakage. *Geophysical Research Letters* 41(4), 1238–1246. <https://doi.org/10.1002/2014GL059278>.
- Chaisson, W.P., Ravelo, A.C., 1997. Changes in upper water column structure at Site 925, late Miocene-Pleistocene: Planktonic foraminifer assemblage and isotopic evidence. *Proc. Ocean Drilling Prog., Scientific Results* 154, 255–268.
- Darby, D.A., 2008. Arctic perennial ice cover over the last 14 million years. *Paleoceanography* 23, 1 07. <https://doi.org/10.1029/2007PA001479>.
- De Schepper, S., Gibbard, P.L., Salzmann, U., Ehlers, J., 2014. A global synthesis of the marine and terrestrial evidence

- for glaciation during the Pliocene Epoch. *Earth Science Rev* 135, 83–102. <https://doi.org/10.1016/j.earscirev.2014.04.003>.
- De Schepper, S., Groeneveld, J., Naafs, B.D.A., Renterghem, C., Hennissen, J., Head, M.J., Louwye, S., Fabian, K., 2013. Northern Hemisphere glaciation during the globally warm early Late Pliocene. *PLoS ONE* 8(12), 81508. <https://doi.org/10.1371/journal.pone.0081508>.
- Dolan, A.M., Haywood, A.M., Hill, D.J., Dowsett, H.J., Hunter, S.J., Lunt, D.J., Pickering, S.J., 2011. Sensitivity of Pliocene ice sheets to orbital forcing. *Palaeogeography, Palaeoclimatology, Palaeoecology* 309, 98–110. <https://doi.org/10.1016/j.palaeo.2011.03.030>.
- Dowsett, H.J., Robinson, M.M., Haywood, A.M., Hill, D.J., Dolan, A.M., Stoll, D.K., Chan, W.L., Abe-Ouchi, A., Chandler, M.A., Rosenbloom, N.A., Ottobliesner, B.L., Bragg, F.J., Lunt, D.J., Foley, K.M., Riesselman, C.R., 2012. Assessing confidence in Pliocene sea surface temperatures to evaluate predictive models. *Nature Climate Change* 2, 1–7. <https://doi.org/10.1038/nclimate1455>.
- Fedorov, A.V., Brierley, C.M., Lawrence, K.T., Liu, Z., Dekens, P.S., Ravelo, A.C., 2013. Patterns and mechanisms of early Pliocene warmth. *Nature* 496, 43–49. <https://doi.org/10.1038/nature12003>.
- Gao, C., Mcandrews, J.H., Wang, X., Menzies, J., Turton, C.L., Wood, B.D., Pei, J., Kodors, C., 2012. Glaciation of North America in the James Bay Lowland, Canada, 3.5 Ma. *Geology* 40, 975–978. <https://doi.org/10.1130/G33092.1>.
- Hall, I.R., Hemming, S.R., LeVay, L.J., the Expedition 361 Scientists, 2017. *Proceedings of the International Ocean Discovery Program*. volume 361. <https://doi.org/10.14379/iodp.proc.361.103.2017>.
- Haywood, A.M., Chandler, M.A., Valdes, P.J., Salzmann, U., Lunt, D.J., Dowsett, H.J., 2009. Comparison of mid-Pliocene climate predictions produced by the HadAM3 and GCMAM3 General Circulation Models. *Global and Planetary Change* 66, 208–224. <https://doi.org/10.1016/j.gloplacha.2008.12.014>.
- Haywood, A., Dowsett, H., Dolan, A., 2016. Integrating geological archives and climate models for the mid-Pliocene warm period. *Nature Communications* 7, 10646. <https://doi.org/10.1038/ncomms10646>.
- Haywood, A.M., Hill, D.J., Dolan, A.M., Otto-Bliesner, B.L., Bragg, F., Chan, W.L., Chandler, M.A., Contoux, C., Dowsett, H.J., Jost, A., Kamae, Y., Lohmann, G., Lunt, D.J., Abe-Ouchi, A., Pickering, S.J., Ramstein, G., Aa, R.N., Salzmann, U., Sohl, L.E., Stepanek, C., Ueda, H., Yan, Q., Zhang, Z., 2013. Large-scale features of Pliocene climate: results from the Pliocene Model Intercomparison Project. *Climate of the Past* 9, 191–209. <https://doi.org/10.5194/cp-9-191-2013>.
- Hill, D.J., Dolan, A.M., Haywood, A.M., Hunter, S.J., Stoll, D.K., 2010. Sensitivity of the Greenland Ice Sheet to Pliocene sea surface temperatures. *Stratigraphy* 7, 111–121. <https://doi.org/10.29041/strat.07.2.02>.
- Hill, D.J., Haywood, A.M., Hindmarsh, R.C.A., Valdes, P.J., 2007. Characterizing ice sheets during the Pliocene: evidence from data and models, in: Williams, M., Haywood, A.M., Gregory, F.J., Schmidt, D.M. (Eds.), *Deep-Time Perspectives on Climate Change: Marrying the Signal from Computer Models and Biological Proxies*. The Micropalaeontological Society, Special Publications. The Geological Society, London, p. 517–538. <https://doi.org/10.1144/TMS002.24>.
- Hillenbrand, C.D., Ehrmann, W., 2005. Late Neogene to Quaternary environmental changes in the Antarctic Peninsula region: evidence from drift sediments. *Global and Planetary Change* 45, 165–191. <https://doi.org/10.1016/j.gloplacha.2004.09.006>.
- Jansen, E., Fronval, T., Rack, F., Channell, J., 2000. Pliocene-Pleistocene ice rafting history and cyclicity in the Nordic Seas during the last 3.5 Myr. *Paleoceanography* 15, 709–721. <https://doi.org/10.1029/1999PA000435>.
- Jiménez-Moreno, G., Pérez-Asensio, J.N., Larrasoaña, J.C., Sierro, F.J., Garcia-Castellanos, D., Salazar, Á., Salvany, J.M., Ledesma, S., Mata, M.P., Mediavilla, C., 2019. Early Pliocene climatic optimum, cooling and early glaciation deduced by terrestrial and marine environmental changes in SW Spain. *Global and Planetary Change* 180, 89–99. <https://doi.org/10.1016/j.gloplacha.2019.06.002>.
- Kemp, A.E.S., Grigorov, I., Pearce, R.B., Naveira Garabato, A.C., 2010. Migration of the Antarctic Polar Front through the mid-Pleistocene transition: Evidence and climatic implications. *Quaternary Science Reviews* 29(17-18), 1993–2009. <https://doi.org/10.1016/j.quascirev.2010.04.027>.
- Kennett, J.P., Srinivasan, M.S., 1983. *Neogene Planktonic Foraminifera, A Phylogenetic Atlas*. Hutchinson Ross Pub. Co, Stroudsburg, Pennsylvania.
- Kleiven, H., Jansen, E., Fronval, T., Smith, T., 2002. Intensification of Northern Hemisphere glaciations in the circum Atlantic region (3.5–2.4 Ma)-ice-rafted detritus evidence. *Palaeogeography, Palaeoclimatology, Palaeoecology* 184, 213–223. [https://doi.org/10.1016/S0031-0182\(01\)00407-2](https://doi.org/10.1016/S0031-0182(01)00407-2).
- Knies, J., Matthiessen, J., Vogt, C., Laberg, J.S., Hjelstuen, B.O., Smelror, M., Larsen, E., Andreassen, K., Eidvin, T., Vorren, T.O., 2009. The Plio-Pleistocene glaciation of the Barents Sea-Svalbard region: a new model based on revised chronostratigraphy. *Quaternary Science Reviews* 28, 812–829. <https://doi.org/10.1016/j.quascirev.2008.12.002>.
- Lam, A.R., Leckie, R.M., 2020. Late Neogene and Quaternary diversity and taxonomy of subtropical to temperate planktic foraminifera across the Kuroshio Current Extension, northwest Pacific Ocean. *Micropaleontology* 66(3), 177–268. URL: <https://www.jstor.org/stable/27143634>.
- Levy, R., Cody, R., Crampton, J., Fielding, C., Golledge, N., Harwood, D.M., Henrys, S., McKay, R., Naish, T., Ohneiser, C., Wilson, G., Wilson, T., Winter, D., 2012. Late Neogene climate and glacial history of the Southern Victoria Land coast from integrated drill core, seismic and outcrop data. *Global and Planetary Change* 80-81, 61–84. <https://doi.org/10.1016/j.gloplacha.2011.10.002>.
- Lisiecki, L.E., Raymo, M., 2005. A Pliocene-Pleistocene stack of 57 globally distributed benthic $\delta^{18}\text{O}$ records. *Paleoceanography* 20, 1003, 10 1029 2004 001071. <https://doi.org/10.1029/2004PA001071>.
- Locarini, R.A., Mishonov, A.V., Baranova, O.K., Boyer, T.P., Zweng, M.M., Garcia, H.E., Reagan, J.R., Seidov, D., Weathers, K.W., Paver, C.R., Smolyar, I.V., 2018. *World Ocean Atlas 2018, Volume 1: Temperature*. NOAA Atlas NESDIS 81, 52. URL: <https://archimer.ifremer.fr/doc/00651/76338/>.
- Lunt, D.J., Haywood, A.M., Schmidt, G.A., Salzmann, U., Valdes, P.J., Dowsett, H.J., Loptson, C.A., 2012. On

- the causes of mid-Pliocene warmth and polar amplification. *Earth and Planetary Science Letters* 321–322, 128–138. <https://doi.org/10.1016/j.epsl.2011.12.042>.
- Lutjeharms, J.R.E., 2006. *The Agulhas Current*. Springer, New York.
- Martinez-Boti, M.A., Foster, G.L., Chalk, T.B., Rohling, E.J., Sexton, P.F., Lunt, D.J., Pancost, R.D., Badger, M.P.S., Schmidt, D.N., 2015. Plio-Pleistocene climate sensitivity evaluated using high-resolution CO₂ records. *Nature* 518(7537), 49–54. <https://doi.org/10.1038/nature14145>.
- McClymont, E.L., Elmore, A.C., Kender, S., Leng, M.J., Greaves, M., Elderfield, H., 2016. Pliocene-Pleistocene evolution of sea surface and intermediate water temperatures from the Southwest Pacific. *Paleoceanography* 31(6), 002954. <https://doi.org/10.1002/2016pa002954>.
- McClymont, E.L., Ho, S.L., Ford, H.L., Bailey, I., Berke, M.A., Bolton, C.T., De Schepper, S., G.R., Grant, Groenewald, J., Inghish, G.N., Karas, C., Patterson, M.O., Swann, G.E.A., Thirumalai, K., S.M., White, Alonso-Garcia, M., Anand, P., Hoogakker, B.A.A., Littler, K., Petrick, B.F., Risebrobakken, B., Abell, J.T., Crocker, A.J., de Graaf, F., Feakins, S.J., Hargreaves, J.C., Jones, C.L., Markowska, M., Ratnayake, A.S., Stepanek, C., Tanguan, D., 2023. Climate evolution through the onset and intensification of Northern Hemisphere Glaciation. *Reviews of Geophysics* 61, 2022 000793. <https://doi.org/10.1029/2022RG000793>.
- McKay, R., Naish, T., Carter, L., Riesselman, C., Dunbar, R., Sjunneskog, C., Winter, D., Sangiorgi, F., Warren, C., Pagan, M., 2012. Antarctic and Southern Ocean influences on Late Pliocene global cooling. *PNAS* 109, 6423–6428. <https://doi.org/10.1073/pnas.1112248109>.
- Naish, T., Powell, R., Levy, R., Wilson, G., Scherer, R., Talarico, F., Kriesek, L., Niessen, F., Pompilio, M., Wilson, T., Carter, L., Deconto, R., Huybers, P., McKay, R., Pollard, D., Ross, J., Winter, D., Barrett, P., Browne, G., Cody, R., Cowan, E., Crampton, J., Dunbar, G., Dunbar, N., Florindo, F., Gebhardt, C., Graham, I., Hannah, M., Hansaraj, D., Harwood, D.M., Helling, D., Henrys, S., Hinnov, L., Kuhn, G., Kyle, P., Ufer, A.L.A., Maffioli, P., Magens, D., Mandernack, K., McIntosh, W., Millan, C., Morin, R., Ohneiser, C., Paulsen, T., Persico, D., Raine, I., Reed, J., Riesselman, C., Sagnotti, L., Schmitt, D., Sjunneskog, C., Strong, P., Taviani, M., Vogel, S., Wilch, T., Williams, T., 2009. Obliquity-paced Pliocene West Antarctic ice sheet oscillations. *Nature* 458, 322–328. <https://doi.org/10.1038/nature07867>.
- Nirmal, B., Mohan, K., Tripathi, A., Christensen, B.A., Mortyn, P.G., De Vleeschouwer, D., Prakasam, M., Saravanan, K., 2023. Agulhas leakage extension and its influences on South Atlantic surface water hydrography during the Pleistocene. *Palaeogeog. Palaeoclim. Palaeoeco* 615(7253), 111447. <https://doi.org/10.1016/j.palaeo.2023.111447>.
- Ogg, J.G., 2020. Geomagnetic Polarity Time Scale. *Geologic Time Scale 2020*, 159–192. <https://doi.org/10.1016/B978-0-12-824360-2.00005-X>.
- Orsi, A.H., Whitworth, T., Nowlin, W.D., 1995. On the meridional extent and fronts of the Antarctic Circumpolar Current. *Deep Sea Research Part I: Oceanographic Research Papers* 42(5), 641–673. [https://doi.org/10.1016/0967-0637\(95\)00021-W](https://doi.org/10.1016/0967-0637(95)00021-W).
- Ravelo, A., Andreasen, D., Lyle, M., Lyle, A., Wara, M., 2004. Regional climate shifts caused by gradual global cooling in the Pliocene epoch. *Nature* 429, 263–267. <https://doi.org/10.1038/nature02567>.
- Schiebel, R., Hemleben, C., 2017. *Planktic Foraminifers in the Modern Ocean*. <https://doi.org/10.1007/978-3-662-50297-6>.
- Schlitzer, R., 2022. *Ocean Data View [Software]*. Available from <https://odv.awi.de>.
- Simon, M.H., Arthur, K.L., Hall, I.R., Peeters, F.J.C., Loveday, B.R., Barker, S., Ziegler, M., Zahn, R., 2013. Millennial-scale Agulhas current variability and its implications for salt-leakage through the Indian-Atlantic Ocean Gateway. *Earth Planet. Sc. Lett* 383, 101–112. <https://doi.org/10.1016/j.epsl.2013.09.035>.
- Singh, V.P., Pathak, S., Dwivedi, R., 2023. Reduction in the strength of Agulhas Current during Quaternary: Planktic foraminiferal records for 1.2 million years from IODP Hole U-1474A. *Journal of Climate Change* 9(4), 45 – 52. <https://doi.org/10.3233/JCC230031>.
- Tan, N., Ramstein, G., Dumas, C., Contoux, C., Ladant, J.B., Sepulchre, P., Zhang, Z., De Schepper, S., 2017. Exploring the MIS M2 glaciation occurring during a warm and high atmospheric CO₂ Pliocene background climate. *Earth and Planetary Science Letters* 472, 266–276. <https://doi.org/10.1016/j.epsl.2017.04.050>.
- Taylor-Silva, B.I., Riesselman, C.R., 2018. Polar frontal migration in the warm Late Pliocene: Diatom evidence from the Wilkes land margin, East Antarctica. *Paleoceanography and Paleoclimatology* 33(1), 76–92. <https://doi.org/10.1002/2017PA003225>.
- Teschner, C., Frank, M., Haley, B.A., Knies, J., 2016. Plio-Pleistocene evolution of water mass exchange and erosional input at the Atlantic-Arctic gateway. *Paleoceanography* 31(5), 582–599. <https://doi.org/10.1002/2015PA002843>.
- de la Vega, E., Chalk, T.B., Wilson, P.A., Bysani, R.P., Foster, G.L., 2020. Atmospheric CO₂ during the mid-Piacenzian warm period and the M2 glaciation. *Scientific Reports* 10(1), 11002. <https://doi.org/10.1038/s41598-020-67154-8>.
- Westerhold, T., Marwan, N., Drury, A.J., Liebrand, D., Agnini, C., Anagnostou, E., Barnet, J.S.K., Bohaty, S.M., Vleeschouwer, D.D., Florindo, F., Frederichs, T., Hodell, D.A., Houlbourn, A.E., Kroon, D., Lauretano, V., Littler, K., Lourens, L.J., Lyle, M., Pälike, H., Röhl, U., Tian, J., Wilkens, R.H., Wilson, P.A., Zachos, J.C., 2020. An astronomically dated record of Earth's climate and its predictability over the last 66 million years. *Science* 369(6509), 1383–1387. <https://doi.org/10.1126/science.aba6853>.
- Zahn, R., Lutjeharms, J., Biastoch, A., Hall, I., Knorr, G., Park, W., Reason, C., 2010. Investigating the global impacts of the Agulhas Current. *Eos, Transactions American Geophysical Union* 91(12), 109. <https://doi.org/10.1029/2010E0120001>.